Available online www.jocpr.com

Journal of Chemical and Pharmaceutical Research, 2018, 10(12): 35-50

Research Article

ISSN : 0975-7384
CODEN(USA) : JCPRC5

A Study of Correlation between Nickel-based Alloy Hastelloy-C276 Machining and Cutting Tool Life

Shao-Hsien Chen*

The Graduate Institute of Precision Manufacturing, National Chin-Yi University of Technology, Tai-Chung, Taiwan

---

ABSTRACT

Nowadays the nickel-based material is widely applied in some key industries such as defense, aerospace and chemical equipment, which is mainly featured by high mechanical strength, high hardness, temperature resistance and impact resistance. However, precipitation hardening, grain-boundary strengthening and affinity phenomenon may occur to nickel-based material during processing, which may cause serious abrasion to the cutting tools, and finally degrade the quality. The cutting speed, feeding speed and cutting depth will influence the wear of cutting tool. The study will apply Taylor's tool life equation to establish the life equation for the cutting tool. With rare data related to nickel-based alloy, especially the Hastelloy-C276, to produce qualified products at most based on the minimum cost of cutting tool is the direction that the current industry strives for. The objective of the study is to understand the correlation between different cutting parameters and the Hastelloy-C276 material machining. When the rotating speed S=2800rpm and the feeding speed Ft=0.7(mm/tooth), the life of cutting tool is 0.8 times of that at the feeding speed Ft=0.62 (mm/tooth). Moreover, it aims to work out the optimized cutting parameters that can expand the tool life.

Keywords: Nickel-based; Hastelloy-C276

INTRODUCTION

Hastelloy-C276 is a nickel-chromium-molybdenum wrought alloy added with tungsten. With excellent corrosion resistance, it can be widely applied in adverse environment. The high content of molybdenum alloy grants Hastelloy-C276 with the features of corrosion resistance and oxidation resistance, while the chromium can improve the metal stability and thermal resistance. Welding with low content of carbon is corrosion resistant, so it can prevent carbide precipitation when welding [1].

Hastelloy-C276 shows quantity changing rule of the precipitates and Mo near the grain boundary generated by different aging temperature, heat preservation time, and aging levels under 550, 750 and 800℃. It is mainly because the M6C carbide is precipitated along the grain boundary within short time. Moreover, as the carbide is precipitated continuously, the quantity of Mo near the grain boundary will drop to a minimum value (about 6%), which will then keep rising constantly. Mo content in the nickel-based corrosion-resistant alloy is vital to the corrosion resistance property, so it could simulate the precipitated carbide and the Mo quantity and changing law near the grain boundary under different thermal treatment systems by combining with the Thermo-Calc results, the John-Mel isothermal transformation kinetics and Fick's second law.

Hastelloy-C276 high-temperature alloy will be deformed due to high-temperature tensile under high temperature and strain. The flow stress is reduced with the increase of deformation temperature, but is increased with the increase of deformation rate. When the temperature reaches 700°C, it shows apparent characteristic of steady flow stress, and the alloy deformation mechanism is mainly dynamic recovery. When the temperature reaches 750°C, dynamic recrystallization will occur to the alloy with the increase of strain [2].The main factors of flow stress include the deformation temperature, the strain rate and the basic parameters of chemical components, such as the thermal deformation of plastic deformation. Hastelloy-C276 is the super alloy with high strain deformation [3-4]. The chemical compound in the metal P, μ and the carbide precipitate show different aging situation in Hastelloy-C276[5-7]. As mentioned by Leonard [8], Hastelloy-C276 used in P phase goes through precipitation in heat treatment for several minutes under 875◦C, and μ phase will be transformed into P phase after a long time. Some cutting study conducts analysis and comparison for Ti-6Al-4V and Inconel 718. With the increase of cutting speed, the cutting force shows a reduction trend. It is mainly because the cutting temperature leads to change of cutting force. It is found the cutting force of Inconel 718 is larger than that of Ti-6Al-4V under the same cutting conditions[9]. Thus, it is difficult to machine nickel-based material.When the geometric shape and cutting speed of the cutting tool are changed, it is found that the geometric shape is a key factor that influences the cutting force, while the cutting speed shows minor influence [10]. In the lathe experiment, Inconel 718 is processed from different inclination angles. It is found that the cutting tool life will change with the feeding amount. When the feeding amount is too small, the cutting tool life will be shortened. When the spindle rotation speed, feeding speed and cutting depth are increased, the wear of cutting tool will be increased accordingly. Moreover, the cutting speed will affect the machining stability, and overly fast/slow feeding speed will affect the wear of cutting tool [11].

CUTTING PRINCIPLE AND MATERIAL PROPERTIES

Composition of Nickel-based Material Hastelloy-C276

Hastelloy-C276 is unidirectional super alloy among the nickel-based alloys. Its composition as listed in Table 1 mainly includes the elements of Cr, Mo, Fe and W. It has the property of solid solution strengthening without precipitation hardening, and the structure is as shown in Figure 1. Its Chromium element may easily form the inert gas protection layer, which facilitates the corrosion resistance property of the alloy, and can improve the property of solid solution strengthening. Molybdenum can prevent chemical reaction of the material, whose atom size is larger than that of nickel. Therefore, it has the effect of solid solution strengthening. W has the same effect as Mo, especially the strong effect of solid solution strengthening.

Table 1. Chemical Composition of Hastelloy-C276

Component	Weight %	Component	Weight %
Ni (Wt. %)	57	Co (Wt. %)	1.62
Cr (Wt. %)	15.44	Mo (Wt. %)	15.34
Fe (Wt. %)	5.43	W (Wt. %)	3.67
V (Wt. %)	0.41	Mn (Wt. %)	0.52
C (Wt. %)	0.004	Others (Wt. %)	Si < 0.02; P - 0.005; S < 0.01

Table 2. Physical properties

Densit	Electrical Resistively	Dynamic modulus of elasticity	Thermal conductivity	Specific heat
8.89 g/cm3	1.3 μ Ω-m	229 MPa	10.2 W/m.K	427 J/Kg.K

When Hastelloy-C276 alloy is under the condition of solid solution annealing, the alloy elements may be easily dissolved in the austenite base. The standard solid solution annealing is to heat up uniformly under 1120 (Table 2), and then quench to the ambient temperature quickly, so as to prevent the carbide/embrittlement phase formation. Figure 2 shows the representative microscopic structure of the alloy under solution treatment condition [13].

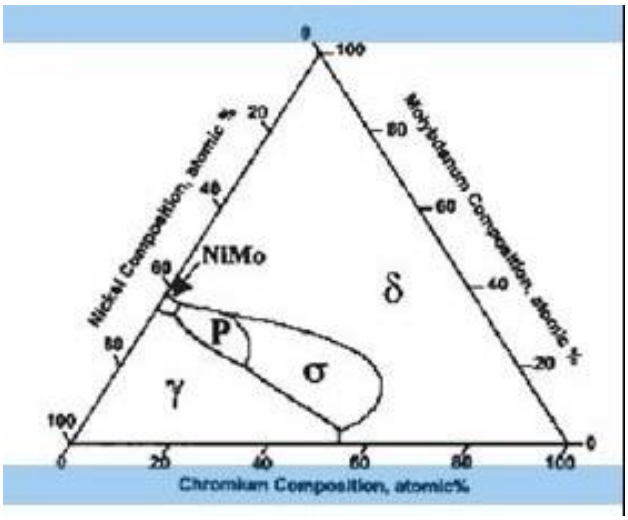

Figure 1. Main Alloy Elements of Hastelloy-C276 Material

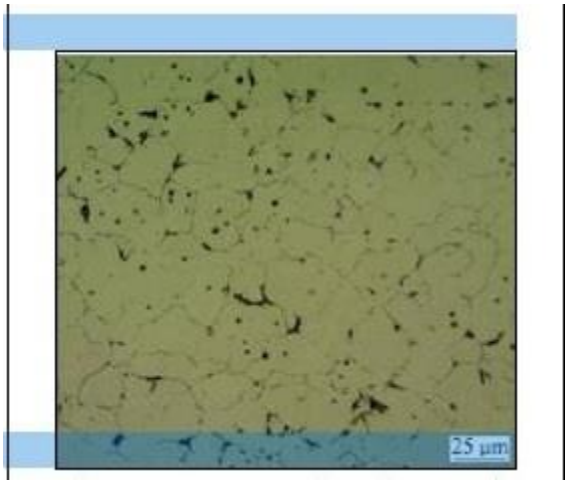

Figure 2. Representative Microscopic Structure of the Alloy

The performance of alloy C-276 may form different mechanical properties under different temperatures and processes[12]. When the temperature change is overly high, it will easily cause the change of phase and mechanical properties. According to the study of Tawancy [7], when the alloy is conducted with aging treatment under 537for a long time, the continuous layer on the grain boundary will form M2C and μ phase precipitation, which will reduce the tensile strength and corrosion resistance.

According to the study of Akhtar et al. [6], after the aging treatment under 850℃, it will form the molybdenum-rich μ phase precipitation, which will reduce the strength of impact resistance. After the aging treatment for 120 hours, it will generate full grain brittle fracture. According to the study of Raghavan et al. [5], when the alloy stays in the temperature range of 650℃ -900℃, it will form three phases through aging treatment. The molybdenum-rich μ phase takes the highest proportion, followed by molybdenum-rich M 6 C carbide with the similar composition as μ phase. Topologically close packed (TCP) phase is precipitated on the grain boundary in the austenite base, such as P phase, μ phase, σ phase and M6C carbide. Therefore, both μ phase and P phase are in TCP phase structure. The TCP phase of the super alloy will degrade the mechanical properties, such as the breaking strength, ductility, as well as the impact resistance and corrosion resistance under the ambient temperature. The high content of MO and W elements in P phase and μ phase can form the solid solution of γ phase (austenite), which is greatly helpful for increasing the tensile strength under high temperature and reducing the anti-elasticity. σ phase of TCP phase can reduce the creep rupture strength and the ductility. To improve the elasticity change and machining degradation, it can add the elements such as Mo and W.

Machining Properties of Nickel-based Material

Generally, there are many variables that influence the cutting properties of the material. The machining can be divided into the following situations as shown in Figure 3[17]. However, in modern cutting history, Hastelloy-C276 material is classified into the type that is hard to cut. The main reasons are listed as below:

High hardening capacity

The strengthening mechanism of nickel-based super alloy takes advantage of coherent precipitation-hardening effect of γ' phase (both γ phase and γ' phase are FCC, with the mechanical property of excellent ductility. Their difference

of lattice constant is about 1%), so the alloy can retain high mechanical strength under high temperature. Moreover, the precipitation-hardening of γ' and γ" shows excellent coherency with the base under high temperature (600~800℃) [16]. Therefore, it still has quite high flow stress under high plastic deformation. The shear zone will generate extremely high strain rate (γ=105) and great plastic deformation (γ=2~5) in the process of cutting. The structure of nickel-based material contains large amount of alloy elements and precipitates. When excessive plastic deformation occurs, it will generate quite high stacking fault, which will increase the flow shear stress greatly.

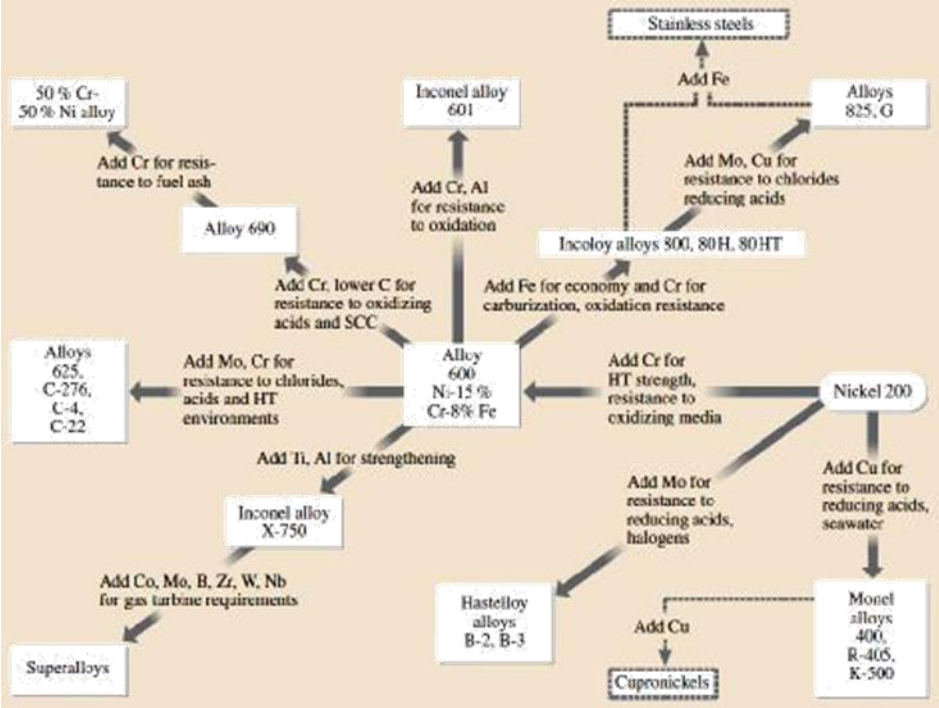

Figure 3. Effects of Alloying Additions on the Corrosion Resistance of Nickel Alloys

Kear Blak Giamei [19]once mentioned that the energy of APB is far greater than that of SISF, SESF and CF when the nickel-based super alloy is under high plastic deformation, as shown in Figure 4 [24]. The large amount of precipitates（γ" phase or γ` phase）in the nickel-based material, namely the solid solution elements, will hinder the movement of dislocations during the plastic deformation. Such precipitates are quite stable under high temperature. Therefore, in the deformation mechanism of Inconel-718, local twinning deformation will be generated due to the difficult movement of dislocations. Therefore, twinning deformation plays a critical role in the plastic deformation of the nickel-based material. However, if the deformation strength under high temperature is improved for the nickel-based material, it may easily cause damage to the cutting tool [14].

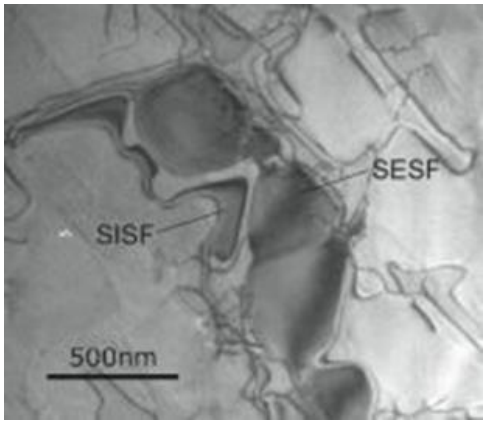

Figure 4. The Ribbon Features Widely Extended SISF and SESF Formed in Successive rows of Γ Precipitates

Low heat conductivity

Most heat generated by cutting nickel-based alloy is not carried by the chips [15], which will be transferred to the cutting tool. Plus the high yield stress and tensile strength, the cutting tool must bear high temperature and high stress. Consequently, it will cause serious abrasion and even cutting edge chipping. Moreover, the nickel-base alloy and the material of cutting tool show high affinity under high temperature, especially the inclined plane where the chips get in contact with the cutting tool will have serious abrasion. That is because the chips flow to the cutting tool through the shear plane, and the friction and temperature on the inclined plane of cutting tool are quite high, which makes Ni diffuse beyond the grain boundary of the adhesive CO on the cutting tool [16]. When the changes of cutting tool reduce the strength, it will cause damage when milling. Besides, it may usually generate build-up edge on the cutting tool. The build-up edge may drop off or re-grow when it is unstable, which may cause local peel-off and even rounding of the cutting tool. Compared with the general iron alloy, the maximum cutting temperature and stress for cutting the nickel-based material are concentrated on the front edge of the contacting plane on the cutting tool, as shown in Figure 2-3. If it is too close to the cutting edge, the cutting edge will bear overly high horizontal stress. When the chips contact the cutting tool for a short time, the strip will be heavily loaded [15]. Plus the high-temperature softening, it may easily cause chipping. The large amount of carbide contained in the nickel-based material will generate cutting effect for the cutting tool, causing abrasion to the flank and face.

Strengthening mechanism of nickel-based super alloy

The nickel-based super alloy has excellent mechanical strength property under high temperature. Its strengthening mechanism will be introduced as below [20-22]:

Solid solution strengthening of austenite base: The solid solution heat treatment for Hastelloy-C276 material includes two processes: (1) Heat up in 1040℃~1150℃; (2) Cool down to the black state quickly around 400℃ within two minutes. After such treatment, the material will possess property of excellent corrosion resistance. The nickel-based super alloy contains about 19% Cr and 3% Mo, for both of which the ion size is much larger than that of Ni. Therefore, when solid solution is in the base, it will be transformed into substitution solid solution. This will generate torture of crystal lattice in the base, so as to achieve strengthening effect.

Precipitation-strengthening γ' and γ": Precipitates of γ' and γ" are regular and coherent. For such precipitates, scholars generally think the strengthening source includes: 1. Reverse boundary and defect hardening caused when the dislocations go through the precipitates; 2. dislocation ring formed the by dislocations passing by or going around the dislocations when the precipitates are large enough; 3. The strength of precipitates when the dislocations go through the precipitates; 4. Coherent strain; 5. Precipitation size and volume ratio, as shown in Figure 5.

Grain-boundary strengthening: It is mainly the strengthening effect of the carbide precipitated on the grain boundary, so as to prevent slippage of the grain boundary. Some boron makes it segregated to the grain boundary, so as to relieve the diffusion trend of grain boundary. In addition, the strengthening effect can be achieved by controlling the direction and size of the grain.

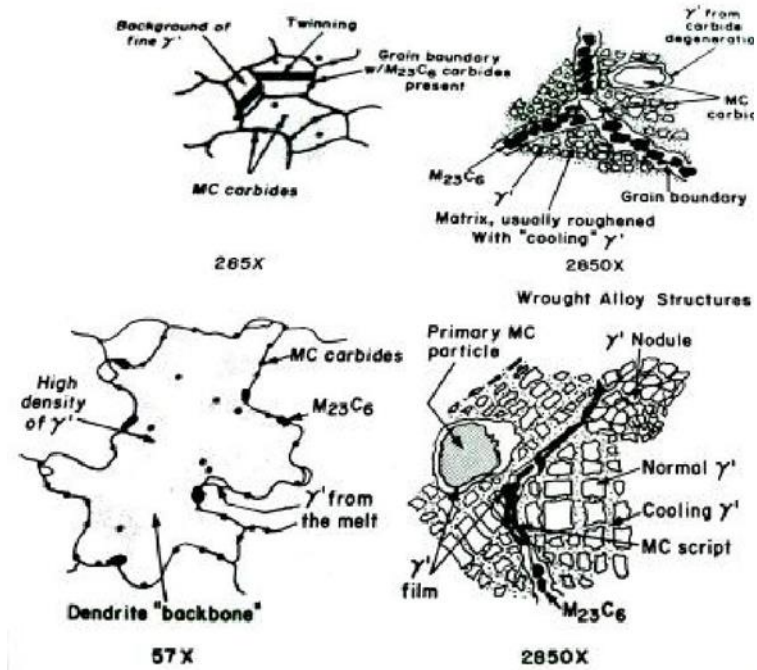

Figure 5. Precipitation-Strengthening Mechanism of Nickel-based Super Alloy

Cutting Tool Life Equation

During the cutting process, the contact between the cutting tool, the chips and the work piece causes the wear to the cutting tool. Generally, the wear of the cutting tool is analyzed and defined based on the accuracy of work piece or the abrasion of the cutting tool. The accuracy of work piece is mainly based on the surface accuracy and geometric accuracy of the work piece. The wear of the cutting tool is mainly attrition and abrasion, including friction, adhesion, diffusion and oxidation wear. Nickel-based material may easily cause diffusion and oxidation wear. The wear type of the cutting tool is mainly flank wear and crater wear on the face. The study applies Taylor's tool life equation to establish the related data, as shown in Figure 6. The equation is as shown below [23]:

$VT^n = C$

When T=1, V=C

$$n = \tan\theta = \frac{\log V_3 - \log V_2}{\log T_2 - \log T_3}$$

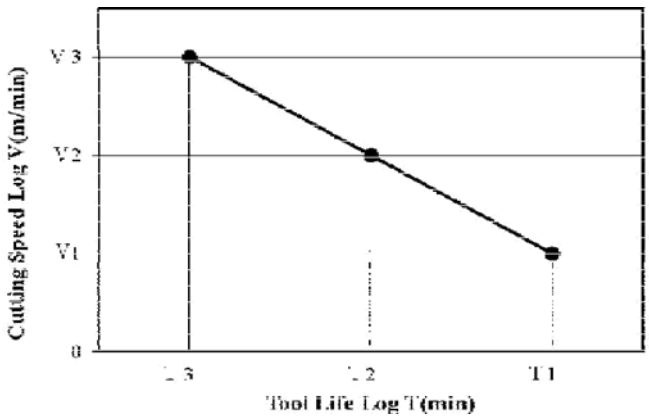

Figure 6. Correlation between Machining Time and Speed

The wear of the cutting tool is mainly due to the following reasons: tool installation and calibration, mechanic vibration, shaft and holder, cutter (material and coating layer), cutting parameters (cutting speed, feeding speed and cutting depth), cutting fluid, work piece (material properties and hardness) etc. The wear can be mainly divided into the following three categories based on different location [23]:

Flank wear: The cutting plane between the flank and the work piece is worn gradually due to the contact during the cutting process. The wear is increased with the cutting speed, as shown in Figure 7. Wear refers to the wear zone width, which can be observed by high-magnification CCD. The change of the in wear zone width can be further divided into the following types, as shown in Figure 8.

Initial wear: The cutting tool is worn fast, because the cutting tool face is rough, and the stress on the cutting edge is concentrated in the initial period. Later wear zone will be formed on the face, so as to reduce pressure and stabilize the wear rate.

Normal wear: The wear zone width is increased uniformly with the time passing by, and the wear condition is stable. It is the effective period of the cutting tool. The normal abrasion curve can be almost considered as linear, and the inclination rate represents the wear rate. Such inclination rate is a key indicator to judge the performance of cutting tool.

Serious wear: The wear of cutting tool enters serious wear stage. In this stage, the cutting force is increased, the temperature keeps rising and the wear rate is increased quickly. The cutting tool will lose the cutting ability very quickly. It should avoid entering this stage because it causes great damage to the cutting tool material.

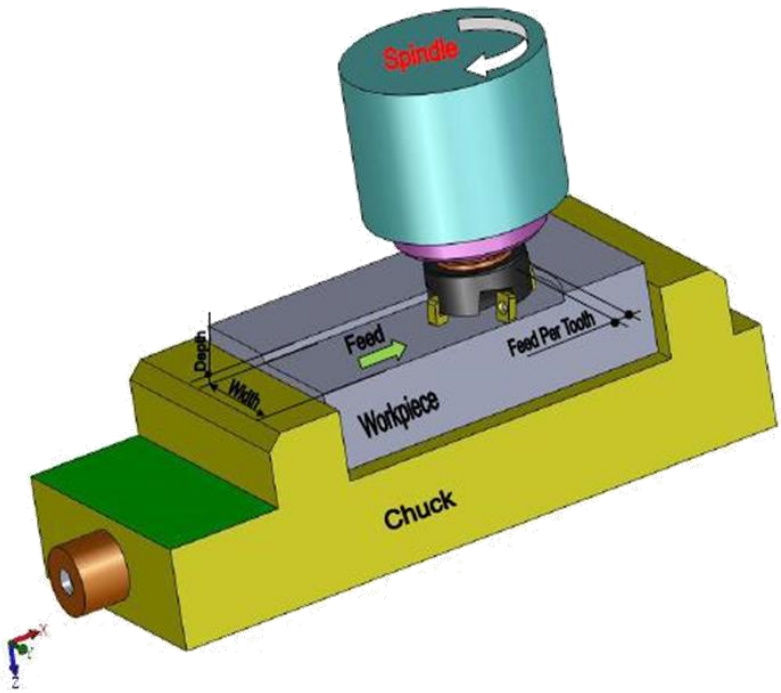

Figure 7. Machining parameters diagram

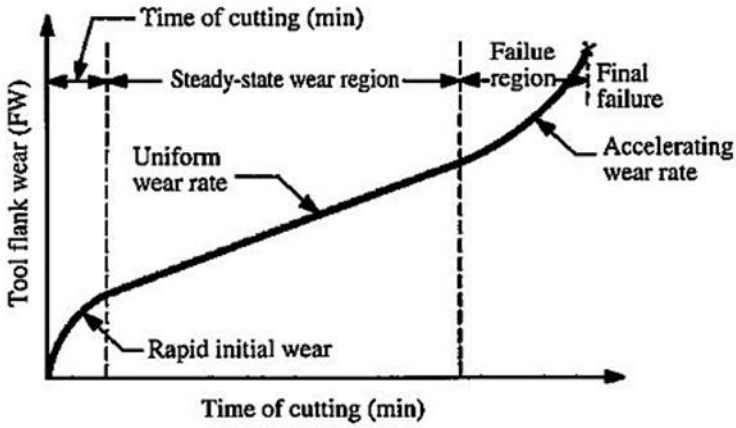

Figure 8. The relationship between the Machining time and the tool life

Experimental Instruments and Planning

The study applies CNC milling machine in the cutting experiment, with the shaft rotation speed is 10000rpm, and power is 11KW, with feeding shaft speed is 36m/min. In terms of the cutting tool, N-class TiAlN multilayer cladding cutting tool is used. Therefore, the cutting tool and the CNC milling machine are fixed in the experiment, with the specification as listed Table 3:

Table 3. Experimental Instruments and Specifications

Name	Properties	Equipment
CNC milling station	X/Y/Z-axis travel: 1020/520/505 mm Main shaft rpm: 10000rpm Main shaft motor power: 7.5/11kW Fast feed speed in X/Y/Z-axis: 40/40/30 m/min	
Cutting Tool	Cutting tool: Seco_XOMX180631 ME13 F40M Holder-specification:R217.69-3232.3-18- 3AN Tool diameter: 32mm	

In the experiment, the fixed factors are down milling, cutting depth dp=0.1 mm and cutting distance L=50 mm, while the variable factors are the feeding rate and cutting speed of each cutting edge. After the feeding speed of each cutting edge is adjusted in each stage, it could change the cutting speed and observe the cutting time. And then substitute into the equation to establish the cutting tool life formula, and conduct comparison and discussion. The experimental planning flowchart is as shown in Figure 9.

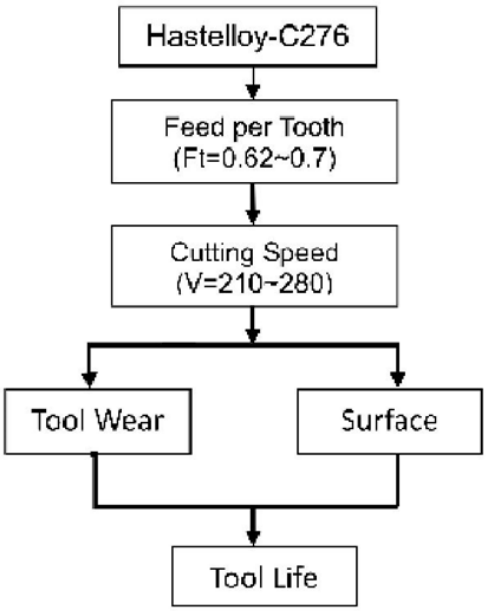

Figure 9. Experimental Flowchart

RESULT AND DISCUSSION

Impact of various parameters on the cutting tool wear

This section presents the observations of the wear found on the cutting tool, which is as shown in Figure 10. When the cutting speed was fixed at V=280 m/min, rpm at S=2800 rpm and feed per tooth at Ft=0.7 mm/toot, the service life of the tool subject to wearing was approximately 0.8 times of that with the feed per tooth at Ft=0.62 mm/tooth.

However, the amount of material removed was the same. With these cutting speed and rpm, therefore, the feeding was faster to produce a greater production efficiency but with relatively the same wearing. If the cutting speed was fixed at V=210 m/min, rpm at S=2100rpm and feed per tooth at Ft=0.62~0.66 mm/tooth, the tool life was 1.6~2 times of that with the feed per tooth at Ft=0.68~0.7 mm/tooth, and the amount of material removed was 1.5 times as much. It is clear that the cutting tool was less worn and more durable when the feed per tooth was set at Ft=0.62~0.66 mm/tooth with lower rpm and cutting speed.

CONCLUSION

The condensation reaction between 5-chloro-4-hydroxy-3-methoxybenzaldehyde and 3-chloro-4-hydroxybenzaldehyde with cyclopentanone were produced 2,5-*bis*(5'-chloro-4'-hydroxy-3'-methoxybenzylidene)cyclopentanone (CHMBC) and 2,5–*bis*(3'–chloro–4'–hydroxybenzylidene)cyclopentanone (CHBC), respectively. The in vitro antioxidant assays demonstrated that curcumin analogues have antioxidant activity, either by DPPH radical scavenging activity and β-carotene bleaching method. The potency of antioxidant activity of CHMBC was more higher than that CHBC, curcumin and pentagamavunon-0 (PGV-0) that measure by the β-carotene bleaching method. While antioxidant activity of curcumin analogues using DPPH radical scavenging assay was lower than that PGV-0 and curcumin.

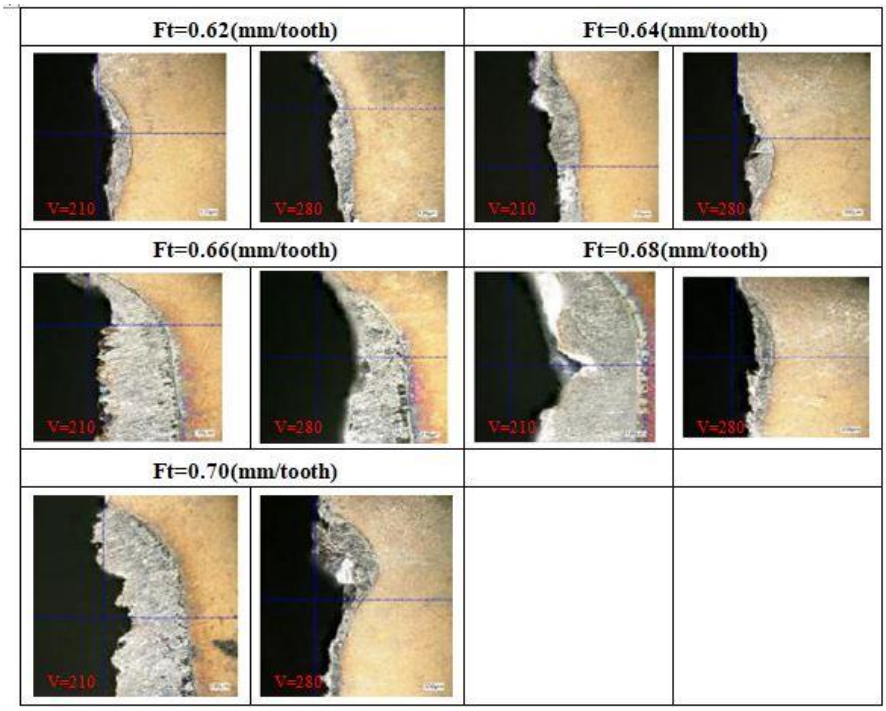

Figure 10. Wearing of the tool

Impact of Various Parameters on Surface Accuracy

The surface roughens is an important result when the Ni-based Hastelloy-C276 is being machined. The major factors that have influence on the surface accuracy are feed per tooth, corner radius, cutting vibration and cutting tool wear. The same tool setup was carried over for the study in order to observe the impact of machining on the wear. As shown in Figure 11, the surface roughness increased with the feed per tooth. The theoretical roughness (Rth) displayed the same trend as the experimental roughness (Rt). It was found in the experiment that the increase of feed

will cause increasing surface roughness and vice versa, At Ft=0.7 the experimental and theoretical values was 40% apart and the percentage was 14% at Ft=0.62. The major factors and the cutting tool wear had mutual influence on one another as shown in the figure above. During the machining of Ni-based materials, therefore, the rapid wearing of cutting tool resulted in the deterioration of machining accuracy. It is imperative to reduce cutting tool wear and establish the data of its service life.

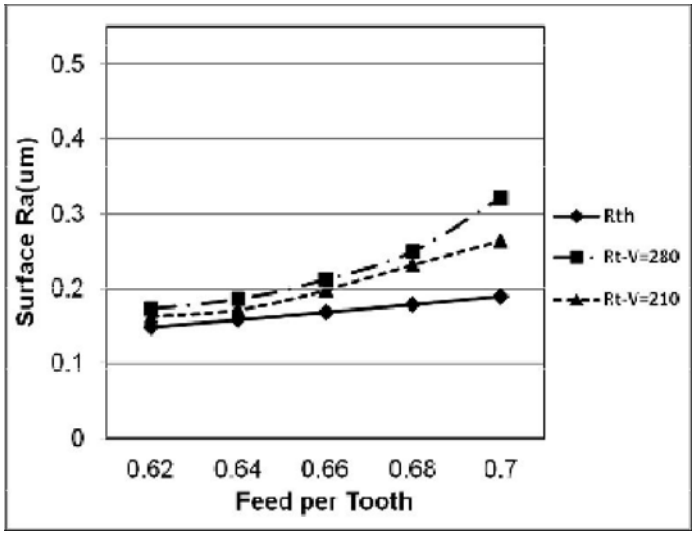

Figure 11. Surface roughness of tested feed per tooth

Establishment of the Tool Life

The Taylor formula was introduced to this study for analysis. The equation of tool life was based on ISO standard. The corresponding tool machining time was identified as the cutting tool wear reached the specified criterion during cutting. The relationship between the number of machining runs and cutting parameters is shown in Figure 12. The greater the cutting speed was, the quicker the experimental travel reached the wearing amount. When the feed per tooth reached 0.70mm/tooth, data were collected to establish the tool life curve as shown in Figure 13.

The tool experienced greater wear when the cutting speed increased because the work hardening and crystal boundary strengthening in the Ni-based material resulted in the rapid wearing in the tool. The slope grew larger as the feed per tooth increased because the increased feed per tooth caused the removal rate to rise which contributed to the increased force acting on the tool and in turn rapidly aggravated the wearing. Table 4 provides the relationship between feed per tooth and tool life and the equations.

For the machining travels and number of machining runs, when the feed per tooth was Ft=0.62, the difference in cutting speed vs. travel was 20% at the greatest. When the feed per tooth was increased to Ft=0.7, the difference in cutting speed vs. travel was 10%, suggesting that the tool wear was less with smaller feed per tooth and the number of machining runs can be increased. With cutting speed fixed at V=210, the difference in feed per tooth was 33%, and the difference was 25% when the cutting speed was raised to V=280. Therefore, the tool wear was less with lower cutting speed, suggesting increased number of machining runs is possible.

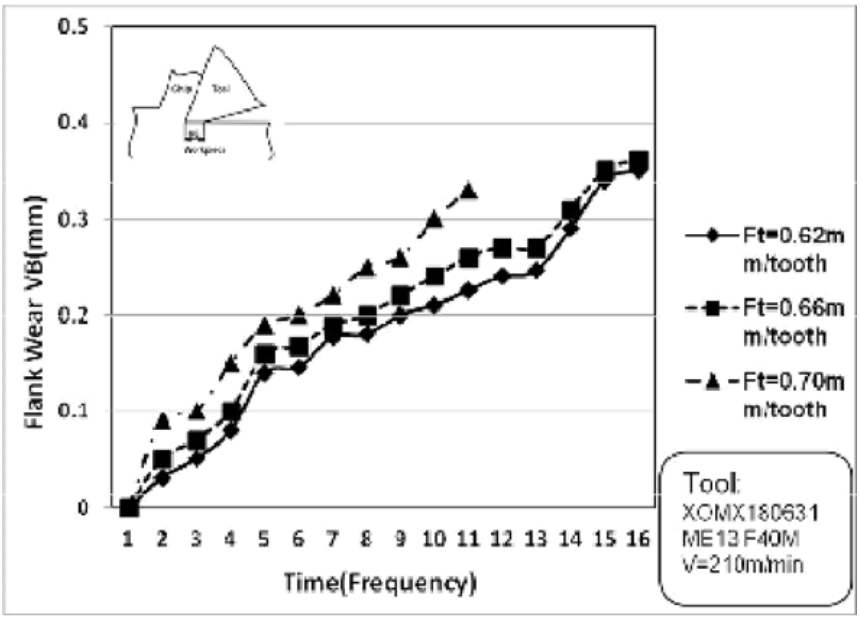

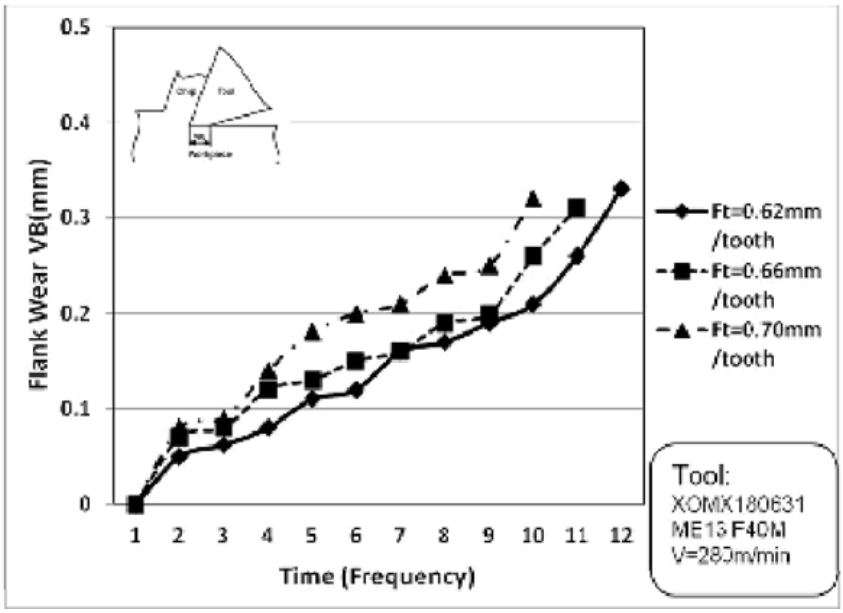

Figure 12. Tool Flank wear of tested times (frequency). (a) V=210m/min and (b)V=280m/min.

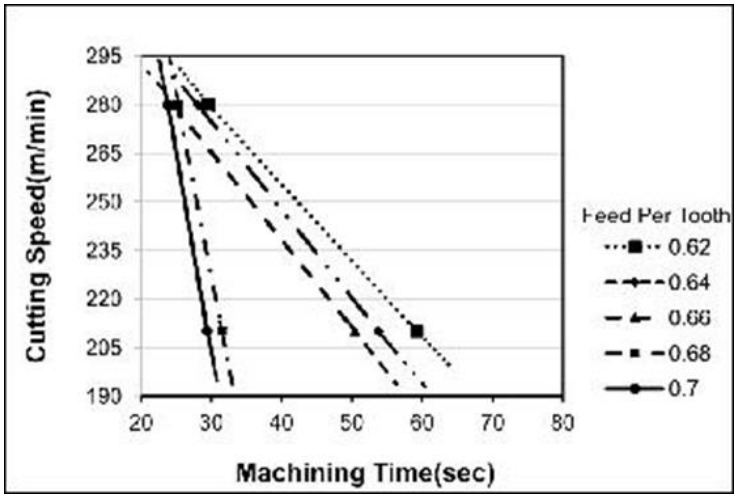

Figure 13. Tool life comparison for different feed per tooth curves

Table 4. Life parameters of square cutter (n, C)

Ft	Tool life parameters (n, C)
0.62	$VT^{0.414}$=208.894
0.64	$VT^{0.832}$=191.773
0.66	$VT^{0.4}$=195.905
0.68	$VT^{1.292}$=91.390
0.70	$VT^{1.363}$=79.537

CONCLUSIONS

1.For surface roughness there are theoretical value and the experimental value. The faster the cutting is, the rougher the surface will be. With Ft=0.7, the experimental value was 40% apart from the theoretical value, and 14% with Ft=0.62. This is probably because the feed per tooth is proportional to the surface accuracy, and the tool wear is also an important factor of influence on the surface accuracy.

2.With the feed per tooth at Ft=0.62 mm/tooth, the cutting speed vs. travel was 20% apart. By increasing the feed per tooth to Ft=0.7, the cutting speed vs. travel was 10% apart, suggesting less tool wear with smaller feed per tooth; i.e. increased number of machining runs is possible. When the cutting speed reached V=210, the feed per tooth vs. travel was 33%. By increasing the cutting speed to V=280, the feed per tooth vs. travel was 25%, indicating less tool wear with lower cutting speed; i.e. increased number of machining runs is possible as well. However, with the feed per tooth at Ft=0.7, the tool was quickly worn to the point that the machining travel had to be reduced.

3.The major machining parameters investigated in this study are presented for interested manufacturers of cutting tool. The tool wears very quickly with the cutting speed at V=280 and feed per tooth at Ft=0.7. This indicates that the parameters have to be brought down to increase the service life of tool when machining the Ni-based Hastelloy-C276.

REFERENCES

[1] JIAO Shao-yang1,ZHU Guan-ni1,DONG Jian-xin1,ZHANG Qing-quan2, Carbide Evolution and Mo Depletion Law in Hastelloy C-276, School of Materials Science and Engineering , University of Science and Technology Beijing.
[2] LU Yan-ling; LIU Jin-xi; LI Xiao-ke; LIANG Jian-ping; LI Zhi-jun; WU Guan-yuan ; ZHOU Xing-tai. *Trans Nonferrous Met Soc China*. **2012,** 22, s84-s88.
[3] MA Yan; LU Dao-gang; MAO Xue-ping; ZHANG Li-yin; CAI Jun. *J Rare Metal Mat Eng*. **2007,** 3, 23-25.
[4] GE Xin-sheng; WU Lei; ZHANG Hai-bo; CUI Jun. *J Pressure Vessel*. **2007,** 3, 23-25.
[5] M Raghavan; BJ Berkowitz; JC Scanlon. *Metall Trans.* **1982,** 13A, 979-984.
[6] JI Akhter; MA Shaikh; M Ahmad; M Iqbal; KA Shoaib; W Ahmad. *J Mater Sci Lett.* **2001,** 20, 333-335.
[7] H.M. Tawancy. *J Mater Sci*. **1981,** 16, 2883-2889.
[8] RB Leonard. *Corrosion*. **1973,** 222-228.
[9] N Fang; Q Wu. *J Mat Processing Technol.* **2009,** 209, 99, 4389.
[10] Muammer Nalbant; Abdullah Altn; Hasan Gökkaya. *Mat Design.* **2006,** 28, 1334-1338.
[11] M Rahman; WKH Seah; TT Teo. *J Mat Processing Technol*. **1997,** 63, 199-204.
[12] LU Yanling; LIU Jinxi; LI Xiaoke; LIANG Jianping; LI Zhijun; WU Guanyuan; ZHOU Xingtai. *Trans Nonferrous Met Soc China*. **2012,** 22, s84−s88.
[13] MJ Perricone; JN Dupont; MJ Cieslak. *Metallurgical Mat Transactions*. **2003,** 34A, 1127-1132.
[14] Basim A Khidhir; B Mohamed. *J Mech Sci Technol*. **2010,** 24(5), 1053-1059.
[15] EO Ezugwu. *J Braz Soc Mech Sci Eng*. **2004.**
[16] Foke AE; Westermamm FE; Kemphans J; Shin WT; och; Hoch M. **1977,** 228-237
[17] Frank G. Springer Handbook of Condensed Matter and Materials Data , *Springer*,**2005**.
[18]Sims CT; Stoloff NS; Hagel WC. Superalloys. NewYork: John Wiley and Sons; **1986.**
[19] Giamei AF; Kear BH. *Metall Trans.* **1970**, 1, 2185.
[20] Li A; Roberts R; Haldipur P; Margetan FJ; Thompson RB. *Rev Prog*. **2003,** 22, 117.
[21] Haldipur P; Margetan FJ; Thompson RB. Rev Progress in QNDE. **2003,** 22, 1355.
[22] Bhadeshia HKDH. Nickel Based Superalloys, University Of CAMBRIDGE.
[23]Milton C. SHOW, Metal Cutting Principle, OXFORD, **1991.**
[24] Vorontsov VA; Voskoboinikov RE; Rae CMF. *Philosophical Magazine Letters*. **2010,** 1-17.